

## Coupled plasmon and phonon in the accumulation layer of InAs(110) cleaved surfaces

Y. Chen, J. C. Hermanson, and G. J. Lapeyre

*Physics Department, Montana State University, Bozeman, Montana 59717*

(Received 15 November 1988)

For the first time, high-resolution electron-energy-loss spectroscopy (HREELS) measurements of the coupled plasmon and phonon modes on *n*-type InAs(110) cleaved surfaces were carried out. Core-level shifts observed in ultraviolet photoemission spectroscopy indicate that an accumulation layer is formed near the surface after the surface is exposed to hydrogen. The HREELS spectra show the evolution of the plasmon due to the accumulation-layer formation and its coupling to the phonon. Spectra of different primary energy were also taken to study the dispersion behavior of the plasmon. A model calculation based on a self-consistent free-carrier profile together with the Debye-Hückel description of the local dielectric response was performed to aid the interpretation of the spectra. Reasonable fits to the data were obtained for surface charge deficits in the range of  $10^{11}$  to  $10^{12}$  electrons/cm<sup>2</sup>. Evidence for a "dead layer" very near the surface was found for each accumulation layer studied. This work supplements earlier studies of coupled plasmon-phonon modes in III-V semiconductors with depletion layers.

### INTRODUCTION

The study of III-V semiconductor surfaces has drawn much attention recently, partly due to their wide application in device technology as well as their interesting physical properties. Of particular interest is the high-resolution electron-energy-loss spectroscopy (HREELS) probe of the space-charge region of the semiconductor. This technique is ideal because its probing depth is on the order of a few hundred angstroms, which is comparable to the width of the space-charge region. Many studies have been carried out.<sup>1-13</sup> However, most of these studies are focused on the plasmon near a depletion layer and its coupling to the optical phonon, since most free semiconductor surfaces can only form a depletion layer. The ZnO(0001) oxygen face has been reported as a strong quantized accumulation layer where a two-dimensional plasmon is observed.<sup>12,13</sup> In this paper, we present the results of a HREELS study of the plasmon in the accumulation layer on the cleaved InAs(110) surface. Unlike ZnO the band bending on this surface is only a few tenths of an electron volt, which produces a weak accumulation layer. The spatial extent of this layer is much larger than that of ZnO and is comparable to the probing depth of HREELS. Thus the details of the free-carrier density profile will affect the HREELS spectrum. From this standpoint, our results provide a very good reference for testing theoretical models.

### EXPERIMENTAL PROCEDURES

The experiment was performed with a Leybold-Heraeus model ELS-22 spectrometer. The system also contains low-energy electron diffraction, electron spectroscopy for chemical analysis, and ultraviolet photoemission spectroscopy (UPS). The stainless-steel chamber is pumped by a turbo molecular pump, ion pump, and Ti sublimator. The base pressure was

$1 \times 10^{-10}$  torr during the experiment. The crystal was *n* type with a free-carrier density of about  $1.3 \times 10^{16}$  cm<sup>3</sup> (measured by Hall effect). The cleavage of the crystal was performed by a single wedge technique. The hydrogen exposure was made by using a hot (2000-K) tungsten filament in the chamber, which is not in the line of sight of the sample surface. The dose was recorded as molecular exposure in units of langmuirs (1 langmuir = 1 L =  $1 \times 10^{-6}$  torr sec). The surface Fermi-level pinning was obtained by monitoring the In 4*d* core line shift in the He uv lamp photoemission spectra.

### RESULTS

Figure 1 shows the HREELS spectra of the InAs(110) surface at different stages of accumulation-layer formation achieved by successive hydrogen exposure. The impact energy of the probing electron beam is 21 eV and the angle of incidence is 45°. The scattered electrons are collected in the specular direction. For the clean, cleaved surface, the optical phonon at about 29 meV and its multiple loss and corresponding gain are clearly resolved. The full width at half maximum (FWHM) of the quasielastic peak is about 13 meV. This is significantly larger than that of the top spectrum in Fig. 1 taken on the surface after 20 L of hydrogen exposure. This indicates that the instrumental FWHM is much smaller than 13 meV. The broadening of the quasielastic peak of the clean surface is due to the excitation of the conduction-band plasmon.<sup>5,6</sup> With the electron density of  $1.3 \times 10^{16}$  cm<sup>-3</sup> in our sample, the surface plasmon energy is about 7 meV. Considering the fact that the electrons are depleted from the surface even when the band is flat,<sup>2,3,7-11</sup> the plasmon energy will shift to smaller energy. Thus the plasmon loss is buried in the quasielastic peak. When as little as 1 L of hydrogen exposure is made, surface plasmon excitation produces a very high wing on each side of the elastic peak and the phonon is damped, see

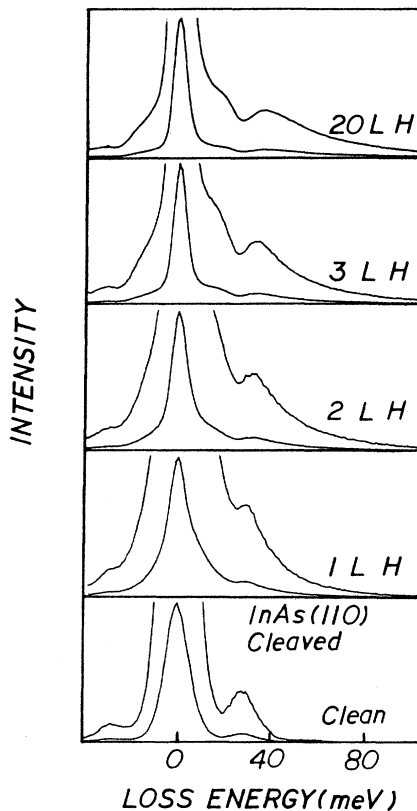


FIG. 1. HREELS spectra of an *n*-type InAs(110) clean, cleaved, and hydrogen-exposed surface. The primary beam energy is 21 eV and the angle of incidence is 45°.

Fig. 1. With 2 L hydrogen, the plasmon can be resolved as a bump and the phonon moves towards higher energy. As hydrogen exposure increases both peaks move toward higher energy and are stable at about 20 L. At the saturation stage, the plasmon and phonon are strongly coupled and it is not possible to identify the losses as simple plasmon or phonon.<sup>11</sup>

The behavior of these coupled plasmon-phonon modes is distinguished from earlier results on GaAs(110) where depletion-layer formation is employed to interpret the data.<sup>7,11</sup> For an *n*-type InAs(110) surface, the Fermi level is reported to pin at 0.13 eV above the conduction-band bottom during oxygen uptake.<sup>14</sup> In our UPS measurement following hydrogen adsorption, a downward band bending of about 0.2 eV is obtained. Therefore, the InAs(110) surface provides one of a very few examples of an accumulation layer on a free surface. The spectra in Fig. 1 can be easily understood if one associates them with the accumulation-layer formation process by which the development of the plasmon loss is directly related to the electron density increase in the accumulation layer as hydrogen is exposed.

The plasmon observed in our experiment clearly behaves like a three-dimensional excitation. This is in contrast to the results of the ZnO(0001) surface<sup>12,13</sup> where the band bending is as large as 1.5 eV. Such a deep

potential will ensure a very strong and narrow accumulation layer<sup>13</sup> which can produce a two-dimensional (subband) plasmon. The typical width of the accumulation layer in this case is on the order of 10–20 Å. The large effective mass ( $0.25m_e$ ) also contributes to the narrowing. However, for InAs(110), the band bending is only 0.2 eV and the effective mass is ten times smaller ( $0.022m_e$ ), providing a typical accumulation-layer thickness of  $d = 100$  Å. For the impact energy used in the experiment, (e.g., about 21 eV) the characteristic momentum transfer parallel to the surface  $k$  is equal to  $\omega/v$ , where  $v$  is the velocity of the probing electron and  $\hbar\omega$  is the typical loss of about 40 meV in our case. With  $k$  evaluated as  $2 \times 10^5 \text{ cm}^{-1}$ , the plasmon extends over a range characterized by  $k^{-1} = 500$  Å. Accordingly the plasmon should not be treated as two dimensional.<sup>15,16</sup>

Another interesting feature is that on the surface with an accumulation layer formed the widths of the two losses are much larger than the quasielastic peak. With the mobility of about  $18500 \text{ cm}^2/v$ , the Drude damping constant is approximately 2–3 meV. This is obviously too small to account for the width. Two possible contributions are discussed here. First, the charge density in the accumulation layer is highly nonuniform while the thickness of this layer is comparable to the probing depth of the incoming electron. Thus, the details of the charge density profile will affect the spectrum. From the standpoint of local response theory, if one divides the space-charge region into sublayers, the local plasmon in each sublayer will be at different energy due to electron density differences. The overall plasmon loss is the envelope of these sublayer plasmons including the interference among them.<sup>11</sup> The second contribution to the plasmon width is due to the instrumental limitation. In the HREELS measurement, due to the finite analyzer collecting slit, the  $k$  transfer is not unique; instead it spreads over a finite range. If the plasmon has a very strong dispersion, the plasmon loss will also be broad.

Figure 2 shows the spectra obtained after the surface was exposed to 100 L of hydrogen; the primary energy  $E_I$  was raised between 1 and 47 eV. This set of curves utilizes the tunability of the probe depth in HREELS to study the spatial localization of the loss features. Noting that the probe depth  $k^{-1} \sim E_I^{1/2}$  we see that low-energy primary electrons tend to excite surface-localized modes. At high primary energies, the spectra reveal modes whose spatial extents are larger. Thus at primary energies below 5 eV, Fig. 2 contains a single loss peak near 29 meV whose width is about equal to the instrumental resolution; this peak is attributed to the unscreened optical phonon and will be discussed in more detail later.

Figure 3 shows the full-energy-range HREELS spectrum of the InAs(110) surface after 100 L hydrogen exposure. The spectrum indicates no noticeable adsorption of molecular hydrogen nor the presence of any significant contamination.

Our interpretation of the spectra displayed in Figs. 1 and 2 is based on model calculations we carried out in the spirit of Lambin *et al.*<sup>17</sup> The latter authors derived an effective surface dielectric function  $\xi_0(k, \omega)$  assuming a local dielectric response of the medium and a classical

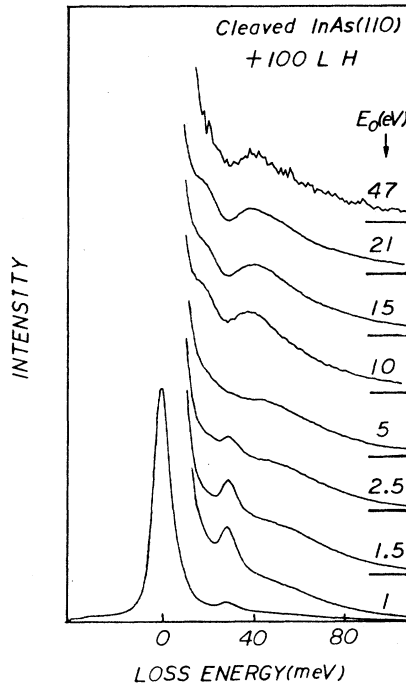


FIG. 2. HREELS spectra of an InAs(110) cleaved surface exposed to 100 L H with different primary energies. The angle of incidence is 45°.

electron trajectory. Here  $k$  and  $\omega$  are the two-dimensional wave vectors parallel to the surface and the frequency. In terms of  $\xi_0$  the "classical" energy-loss probability is given by<sup>17</sup>

$$p_{cl}(\omega) = \frac{4}{\pi^2} \frac{e^2}{\hbar v_n} \int d^2k F(\mathbf{k}, \omega) \text{Im} \frac{-1}{\xi_0(k, \omega) + 1}, \quad (1)$$

where  $v_n$  is the component of the primary electron velocity normal to the surface and the kinematic factor is

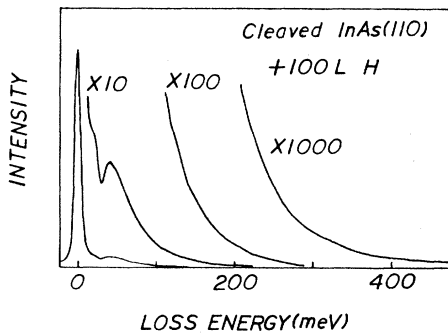


FIG. 3. HREELS spectrum of an InAs(110) surface with 100 L H exposure. The primary energy is 21 eV and the angle of incidence is 45°.

$$F(\mathbf{k}, \omega) = \frac{kv_n^3}{[(\omega - \mathbf{k} \cdot \mathbf{v})^2 + (kv_n)^2]^2}. \quad (2)$$

Omitting multiple excitations the full energy-loss probability can be written as

$$P(\omega) = [1 + n(\omega)] P_{cl}(\omega), \quad (3)$$

where

$$n(\omega) = [\exp(\hbar\omega/k_B T) - 1]^{-1} \quad (4)$$

is the Bose-Einstein occupancy at temperature  $T$ . Thus the loss spectrum for single excitation of plasmon-phonon modes is determined once  $\xi_0(k, \omega)$  is known. In our calculations, we do not restrict the  $k$  integration in (1) since for dipole-allowed processes the scattered electron emerges very near the specular direction (within a few tenths of a degree) and the detector window is about 2° wide. We turn now to the determination of  $\xi_0$ .

Following Ref. 17 we introduce the quantity

$$\xi(k, w, z) = \frac{\epsilon(k, w, z)}{kV(k, w, z)} \frac{\partial V(k, w, z)}{\partial z}, \quad (5)$$

where  $\epsilon$  is the local dielectric function of the medium at depth  $z$  below the surface and  $V$  is the polarization potential. We emphasize that  $k$  is the two-dimensional wave vector as in (1). With  $\epsilon$  a function of  $z$ , Poisson's equation for  $V$  can be written in terms of  $\xi$  as the Riccati equation<sup>17</sup>

$$\frac{1}{k} \frac{d\xi}{dz} + \frac{\xi^2}{\epsilon} = \epsilon. \quad (6)$$

We have solved this equation numerically for various models of  $\epsilon(k, \omega, z)$  using the boundary condition that  $\xi$  is the bulk dielectric function far below the accumulation region. The function  $\xi_0$  needed for (1) is given by

$$\xi_0(k, w) = \xi(k, w, z=0). \quad (7)$$

We now specify the dielectric model used to describe the local response in  $n$ -type InAs(110). Because the bulk free-carrier concentration is low (about  $1.3 \times 10^{16} \text{ cm}^{-3}$ ) the electron gas is nondegenerate. Thus we have used the Debye-Hückel dielectric susceptibility<sup>18</sup>

$$\chi_{DH}(k, w, z) = \frac{4\pi n(z)e^2}{m^* \omega^2} \left[ 1 + \frac{3k^2 k_B T}{m^* \omega^2} \right], \quad (8)$$

where  $n(z)$  is the free-carrier profile,  $m^*$  is the conduction-electron effective mass, and  $\omega$  contains a small imaginary part to account for electron-impurity lifetime effects (the associated energy broadening, determined from the mobility, is about 2.4 meV FWHM). While  $\chi_{DH}$  predicts the plasmon excitations, the phonon contribution to HREELS is contained in the term

$$\chi_{ph}(\omega) = \frac{(\epsilon_\infty - \epsilon_0)\omega_{TO}^2}{\omega_{TO}^2 - \omega^2}. \quad (9)$$

Parameters used in (9) are the dielectric constants  $\epsilon_\infty = 12.3$  and  $\epsilon_0 = 14.9$ , the TO-phonon frequency  $4.1 \times 10^{13} \text{ sec}^{-1}$  or 26.9 meV in energy units, and a small

imaginary part, 1 meV in energy units, supplementing  $\omega$  in the denominator. The full dielectric function needed for (6) is

$$\epsilon(k, \omega, z) = \epsilon_\infty + \chi_{\text{DH}}(k, \omega, z) + \chi_{\text{ph}}(\omega). \quad (10)$$

The  $z$  dependence of  $\epsilon$  is entirely due to  $n(z)$ .

Before turning to the method used to obtain  $n(z)$ , we would like to comment on the validity of the Debye-Hückel susceptibility for our system. Note that the HREELS wave-vector scale determined from the kinematic factor (2) is  $k \approx \omega/v$ , which is an order of magnitude less than the Debye wave vector within the accumulation layer. Hence the long-wavelength approximation (8) is justified.

The free-carrier profile  $n(z)$  was determined from self-consistent solutions of the Schrödinger and Poisson equations appropriate to a jelliumlike model of the conduction electrons.<sup>19</sup> The parameters that specify the model are the effective mass  $m^*$ , the static dielectric constant, the bulk carrier density  $n_0$ , and the surface charge deficit  $Q$ , which ranged from 0 to  $1.5 \times 10^{12}$  electrons/cm<sup>2</sup>. A sine-wave basis<sup>20</sup> of 20–40 states was used to expand the wave function in a finite slab simulating InAs(110); the thickness of the slab was 1600 Å, much larger than the thickness of the accumulation layer, about 100 Å. Symmetry considerations were used to decrease the diagonalization time of the Hamiltonian matrix. We used a convergence-factor technique in which a fraction of the difference potential (output minus input) was added to the input potential at one iteration to define the input potential for the next iteration. Convergence of the potential to within 1 part in  $10^4$  everywhere could be obtained in less than 5 min on an Intel 80386-based personal computer. The energy-loss spectrum was then predicted by solving Eqs. (1) and (6). The greatest source of uncertainty in the results originates in the local dielectric picture itself. Indeed, the Debye screening length is comparable to the thickness of the accumulation layer, so nonlocal dielectric response may be important in principle.<sup>10</sup> Nonetheless, our model results allow us to make a simple, consistent interpretation of the HREELS data in Figs. 1 and 2.

The carrier profile  $n(z)$  we found for the strongest accumulation layer ( $Q = 1.2 \times 10^{12}$  electrons/cm<sup>2</sup>) is shown in Fig. 4. The length unit is the thermal wavelength

$$\lambda = \left[ \frac{\hbar^2}{2m^*k_B T} \right]^{1/2} \approx 81.8 \text{ \AA} \quad (11)$$

at a temperature of 300 K. Note that the carrier density plotted in this figure contains the factor  $\lambda^3$ ; in conventional units,  $n(z)$  has a peak value of  $8 \times 10^{17}$  cm<sup>-3</sup> at a depth of 78 Å. Despite having high density, the electron gas is nondegenerate because the Fermi level, determined from the bulk density, is below the conduction-band minimum.

Calculated HREELS spectra, including a simulated 9-meV FWHM instrumental broadening, are displayed in Fig. 5. The parameter labeling the curves is  $Q$ , the surface charge deficit (positive for an accumulation layer).

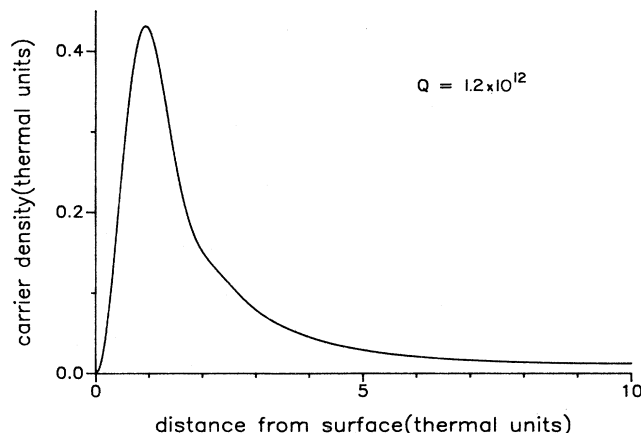


FIG. 4. The charge density profile  $n(z)$  of our self-consistent calculation. The surface charge deficit used is  $1.2 \times 10^{12}$  electrons/cm<sup>2</sup>, which corresponds to 0.26 eV band bending.

Loss features in this figure have a clear correspondence with HREELS features in Fig. 1: (1) when  $Q = 0$  (no accumulation layer) a surface phonon mode is seen at about 29 meV with a width due to the instrumental broadening; (2) as  $Q$  increases, the surface phonon mode broadens and shifts to higher energy, reaching 38 meV when  $Q = 1.2 \times 10^{12}$ ; (3) on the low-energy side of the phonon peak, a plasmon peak emerges from the quasielastic region when  $Q$  reaches  $6 \times 10^{11}$  cm<sup>-2</sup>; the plasmon and phonon peaks move in a roughly parallel fashion as  $Q$  is increased further. In fact, the two peaks seen when  $Q > 0$

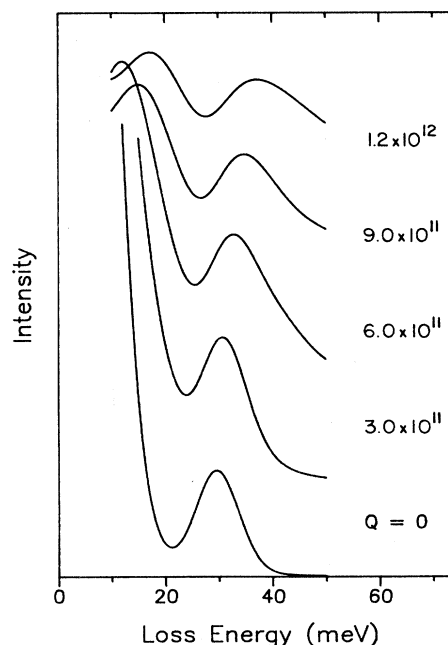


FIG. 5. Calculated spectra with different surface charge deficit and fixed primary energy 21 eV.

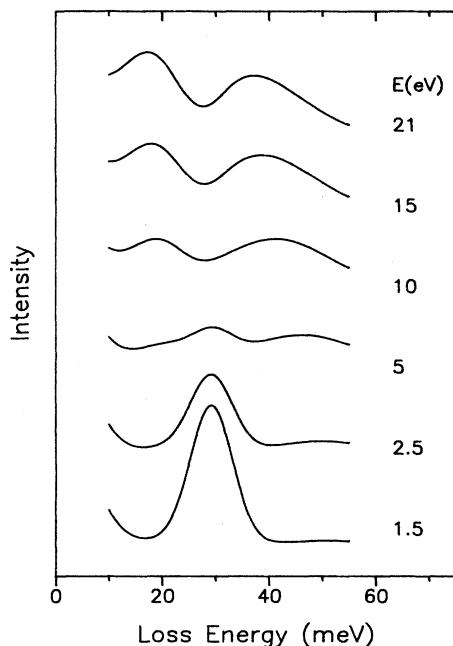


FIG. 6. Calculated spectra with different primary energy and fixed surface charge deficit of  $1.2 \times 10^{12}$  electrons/cm<sup>3</sup>.

are more properly attributed to mixed plasmon-phonon modes. The phonon character of the higher peak decreases as it moves toward higher energy, while that of the lower peak increases. We do not discuss the quasi-elastic peak behavior because we have not included multiple excitations in our calculations. The strongest accumulation layer,  $Q = 1.2 \times 10^{12}/\text{cm}^{-2}$ , corresponds to a band bending of 0.26 eV, in good agreement with our UPS determination of about 0.2 eV for this quantity at 20 L hydrogen exposure.

The broadening and shifting of the plasmon-phonon modes can be understood as follows. When  $Q$  increases so does  $n(z)$  in the accumulation layer; as a result the characteristic plasmon energy increases. Also, the increasing steepness of  $n(z)$  implies a wider range of local plasmon energies, leading to a broadening of the loss features. As mentioned earlier, our finite collector aperture also contributes to the broadening of plasmon features because of dispersion. In our calculations, a separate *unscreened* phonon mode is always seen at 29.4 meV if the broadening parameter is set to zero. Because it is weak, however, this peak merges with the nearby plasmon-phonon mode when broadening is included. Only at  $Q = 0$  does Fig. 5 contain a peak at the unscreened phonon energy. In this case, the weak background charge,  $1.3 \times 10^{16} \text{ cm}^{-3}$ , does not lead to surface plasmon excitations above 10 meV.

Figure 6 displays calculated spectra at  $Q = 1.2 \times 10^{12} \text{ cm}^{-2}$ , corresponding to the hydrogen-saturated surface

studied in Fig. 2. Both figures are labeled with the primary energy  $E_I$ , which was scanned in order to study the localization of the observed modes. When  $E_I < 5$  eV, both the theoretical and experimental spectra contain an unscreened-phonon peak near 30 meV. Since this peak is stronger at low  $E_I$  (small probe depth) we assign it to a phonon mode in the dead layer within 50 Å seen in Fig. 4. This layer of sharply reduced carrier density is a feature of all models that require the electron wave function to vanish at the surface.<sup>19</sup> Apparently the accumulation layer itself screens the bulk of the sample so that at the highest energies (large probe depth) the unscreened phonon cannot be seen in the broadened spectrum. Instead, for primary energies above 5 eV two coupled plasmon-phonon modes are seen in Figs. 2 and 6. Their dispersion is weak because the field of the incoming electron samples a region that is large compared with the thickness of the accumulation layer. On the other hand, note the strong dispersion of the high-energy mode for  $E_I < 10$  eV; though weak it shifts from 40 to about 55 meV as the probe depth is decreased, i.e., as  $E_I$  is decreased. Presumably this behavior is due to the increased effective carrier density when the probe depth is reduced. The calculated spectra in Fig. 6 replicate the data curves of Fig. 2 well, except that the unscreened phonon peak in Fig. 6 persists for primary energies as large as 5 eV. We emphasize that only the kinematic parameter  $E_I$  was varied within the set of theory curves; all material parameters were fixed. The agreement between theory and experiment is surprisingly good, considering that nonlocal corrections to dielectric response<sup>10</sup> may be large for this system.

## CONCLUSIONS

Using HREELS, we studied the coupled plasmon and phonon modes in the accumulation layer of the InAs(110) cleaved surface. The evolution of these two modes during accumulation-layer formation was followed and can be understood in terms of the increasing electron density in the space-charge region. Spectra with different primary energies revealed spatially localized loss features. A theoretical model based on a self-consistent free-carrier profile together with the Debye-Hückel description of the local dielectric response was used to fit the experimental data and good agreement was obtained. Thus even in this case of a strong spatially nonuniform electronic system, the local dielectric theory provides a useful framework for interpreting HREELS data.

## ACKNOWLEDGMENTS

We express our appreciation for the support of J. R. Anderson and M. Jaehnig. This research is supported by the National Science Foundation, Grant No. DMR-8309460.

- <sup>1</sup>A. Pinczuk, G. Abstreiter, R. Trommer, and M. Cardona, *Solid State Commun.* **21**, 959 (1977).
- <sup>2</sup>R. Matz and H. Lüth, *Phys. Rev. Lett.* **46**, 500 (1981).
- <sup>3</sup>A. Ritz and H. Lüth, *Phys. Rev. Lett.* **52**, 1242 (1984).
- <sup>4</sup>Z. J. Gay-Grychowski, R. G. Edgell, B. A. Joyce, R. A. Stradling, and K. Woodbridge, *Surf. Sci.* **186**, 482 (1987).
- <sup>5</sup>Joseph A. Stroscio and W. Ho, *Phys. Rev. Lett.* **54**, 1573 (1985).
- <sup>6</sup>L. H. Dubois, B. R. Zegarski, and B. N. J. Persson, *Phys. Rev. B* **5**, 9128 (1987).
- <sup>7</sup>Yu Chen, Yabo-Xu, and G. J. Lapeyre, *J. Vac. Sci. Technol.* (to be published).
- <sup>8</sup>A. Stahl, *Surf. Sci.* **134**, 297 (1983).
- <sup>9</sup>W. L. Schaich, *Surf. Sci.* **122**, 175 (1982).
- <sup>10</sup>D. H. Ehlers and D. L. Mills, *Phys. Rev. B* **36**, 1051 (1987).
- <sup>11</sup>Y. Chen, S. Nannarone, J. Schaefer, J. C. Hermanson, and G. J. Lapeyre, *Phys. Rev. B* **39**, 7653 (1989).
- <sup>12</sup>A. Many, I. Wagner, A. Rosenthal, J. I. Gersten, and Y. Goldstein, *Phys. Rev. Lett.* **46**, 1648 (1981).
- <sup>13</sup>J. I. Gersten, I. Wagner, A. Rosenthal, Y. Goldstein, A. Many, and R. E. Kirby, *Phys. Rev. B* **29**, 2458 (1984).
- <sup>14</sup>H. U. Baier, L. Koenders, and W. Mönch, *Solid State Commun.* **58**, 327 (1986).
- <sup>15</sup>H. Ibach and D. L. Mills, *Electron Energy Loss Spectroscopy and Surface Vibrations* (Academic, New York, 1982).
- <sup>16</sup>L. H. Dubois, G. P. Schwartz, R. E. Camley, and D. L. Mills, *Phys. Rev. B* **29**, 3208 (1984).
- <sup>17</sup>Ph. Lambin, J. P. Vigneron, and A. A. Lucas, *Phys. Rev. B* **32**, 8203 (1985).
- <sup>18</sup>A. L. Fetter and J. D. Walecka, *Quantum Theory of Many-Particle Systems* (McGraw-Hill, New York, 1971), p. 307.
- <sup>19</sup>D. H. Ehlers and D. L. Mills, *Phys. Rev. B* **34**, 3939 (1986).
- <sup>20</sup>S. R. Streight and D. L. Mills, *Phys. Rev. B* **37**, 965 (1988).